1 The New Era of Biology In Singulo

Taekjip Ha*†‡ and Paul R. Selvin*†

*Department of Physics, †Center for Biophysics and Computational Biology, University of Illinois, Urbana-Champaign, Urbana, Illinois 61801; ‡Howard Hughes Medical Institute, Urbana, Illinois 61801

Many biological reactions are too complex to fully comprehend through the use of conventional ensemble techniques. At the most fundamental level, all biological reactions occur via the action of single enzymes, DNA molecules, or RNA molecules. Studying one biological macromolecule at a time, or biology in singulo, can provide us with extraordinarily clear and often surprising views of these molecules in action.

Single-molecule study of biological processes is a relatively new endeavor, less than 20 years in its entire history (if we exclude single-channel recording, which has long been established as a mainstay in physiology), and has been undergoing an explosive growth of late. For example, the number of publications in the field is growing exponentially, with a doubling time of 2.2 years (Cornish and Ha 2007). If the trend continues indefinitely, in 25 years, every paper in biomedical sciences will include single-molecule data! But, at present, single-molecule techniques are still difficult to master, and major research findings are coming from a small number of research groups. We believe that this will change as single-molecule techniques become "commoditized." We hope that this manual will help to get the techniques out of the labs of specialists into the hands of the general biomedical research community.

Two broadly defined categories of single-molecule methods are (1) fluorescence imaging and spectroscopy and (2) force-based manipulation and detection. We divided the fluorescence part into two, in vitro and in vivo (i.e., living cells). Single-molecule force techniques are also divided into use of optical trap, magnetic trap, atomic force microscope, and nanopores.

The first detection of single fluorophores was made at the liquid helium temperature via absorption (Moerner and Kador 1989) and fluorescence (Orrit and Bernard 1990) and later extended to room temperature (Betzig and Chichester 1993), opening up possibilities for biological applications. What does single-molecule fluorescence tell us about the host biomolecule? First, it tells us that it exists and where it is—in other words, "localization." The presence of a single enzyme or binding of a single ATP molecule to an enzyme can be detected by fluorescence labeling the enzyme or the ATP molecule (Chapter 15). Single-fluorophore localization can be done with about 1-nanometer precision by fitting the image of a single fluorophore (or two fluorophores of different colors) using a two-dimensional Gaussian fit (Chapters 3 and 4). Second, a single fluorophore's polarization response can be used to deduce the orientation of the host molecule or its domain (Chapter 6, and part of Chapter 3). Third, the distance between two fluorophores, a donor and an acceptor, can be deduced by measuring fluorescence resonance energy transfer (FRET) between them. Two primary methods of single-molecule FRET—parallel detection of hundreds of molecules via total internal reflection fluorescence microscopy (TIRFM) and confocal detection of diffusing molecules—are discussed in two separate chapters (Chapter 2 and

Chapter 5, respectively). For TIRFM measurements, the molecule of interest must be tethered to a surface without perturbing its function. Several ways of immobilizing molecules specifically to a surface are discussed in Chapter 20 and in parts of Chapters 2, 3, and 21.

Extending single-molecule detection to living cells is challenging, but it has become possible through the use of (1) very bright quantum dot labeling (Chapter 9), (2) many copies of fluorophores (Chapters 3, 8, and 10), (3) detection by immobilization (Chapter 7), or (4) ingenuous reduction of background fluorescence (Chapter 11). Fluorescence correlation spectroscopy (FCS) is not strictly a single-molecule technique because the signal is averaged over a thousand molecules, but it is performed at "single-molecule" concentrations such that at any given moment, there is one or a few molecules in the detection volume. FCS in vitro and in living cells is presented in Chapter 12.

Optical traps (also called optical tweezers) (Ashkin et al. 1986) can be used to apply force and small movements using a tightly focused laser light. Chapter 13 describes a single-beam or dual-beam optical trap with a few-nanometer resolution, mainly developed for the study of myosin. A subnanometer resolution dual-trap instrument is discussed in Chapter 14. Magnetic traps (also known as magnetic tweezers) (Strick et al. 1996) do not currently have as good a spatial or temporal resolution as optical traps, but they have the important advantage of being able to apply torque and control the supercoiling state of DNA (Chapter 16).

The atomic force microscope (AFM) is primarily used in two different modes, one as an imaging tool (not covered in this manual) and the other as a force transducer/sensor (Chapter 17). The AFM is not as sensitive as optical or magnetic traps in terms of detection of force, but it can apply much higher force, which proves to be ideal for studies of protein folding and unfolding. Finally, nanopores can be made out of natural proteins or fabricated holes in a thin material, and electrical current through the pore can be used to detect transport of DNA and other molecules driven by electrical force (Chapter 18).

What does the future hold for these in singulo techniques? Thus far, most in vitro studies have been limited to relatively simple systems of one molecule or two interacting molecules. However, in the cell, they do not function in isolation. To study more complex molecular machines made of multiple components, techniques must be further developed to measure more than one observable molecule at a time (e.g., measuring multiple distances via three-color FRET [Chapters 2 and 5] or combining force-based methods with fluorescence). Chapter 15 makes inroads toward measuring fluorescence under an optical trap. Ultimately, adding more and more purified components in vitro will reach a point of diminishing return, which is also a natural jumping point to live-cell studies where the cell provides all of the necessary ingredients for physiologically relevant contexts. Technical frontiers will probably be found in either of the two extremes: (1) ultrahigh precision in vitro investigations and (2) live-cell- or even whole-organism-level investigations.

REFERENCES

Ashkin A., Dziedzic J.M., Bjorkholm J.E., and Chu S. 1986. Observation of a single-beam gradient force optical trap for dielectric particles. *Opt. Lett.* **11:** 288–290.

Betzig E. and Chichester R.J. 1993. Single molecules observed by near-field scanning optical microscopy. *Science* **262:** 1422–1425.

Cornish P.V. and Ha T. 2007. A survey of single-molecule techniques in chemical biology. *ACS Chem. Biol.* **2:** 53–61.

Moerner W.E. and Kador L. 1989. Optical detection and spectroscopy of single molecules in a solid. *Phys. Rev. Lett.* **62:** 2535–2538.

Orrit M. and Bernard J. 1990. Single pentacene molecules detected by fluorescence excitation in a *p*-terphenyl crystal. *Phys. Rev. Lett.* **65:** 2716–2719.

Strick T.R., Allemand J.F., Bensimon D., Bensimon A., and Croquette V. 1996. The elasticity of a single supercoiled DNA molecule. *Science* **271:** 1835–1837.

2 Single-Molecule FRET with Total Internal Reflection Microscopy

Chirlmin Joo and Taekjip Ha

Department of Physics and Howard Hughes Medical Institute, University of Illinois, Urbana-Champaign, Urbana, Illinois 61801

ABSTRACT

Single-molecule (sm) fluorescence detection is a powerful method for studying biological events. smFRET (Förster [fluorescence] resonance energy transfer) is now being used to study a variety of biological systems. This chapter focuses primarily on smFRET based on total internal reflection (TIR) microscopy. It begins with discussions of dye choice and labeling of nucleic acids and proteins. These are followed by information on surface preparation and data acquisition. Various methods of data analysis are then presented, as well as information on setting up TIR microscopy, both the objective and the prism types. The chapter ends with a series of protocols that describe the preparation of materials and techniques for imaging and microscopy.

INTRODUCTION

Sm fluorescence detection is a powerful tool in probing biological events without time and population averaging (Weiss 1999; Cornish and Ha 2007). smFRET (single-molecule Förster [fluorescence] resonance energy transfer), first introduced in 1996 (Ha et al. 1996), has been widely adopted by many laboratories around the world to study a variety of biological systems, including DNA, RNA (Zhuang

TABLE 2-1. Explanation of Acronyms and Abbreviations

Acronyms/Abbreviations	Explanation
APD	Avalanche photodiode
BSA	Bovine serum albumin
CV	Column volume
Cys	Cysteine
DM	Dichroic mirror
E	FRET efficiency
E_{app}	Apparent FRET efficiency
EMCCD	Electron multiplying charge-coupled device
FRET	Förster (fluorescence) resonance energy transfer
HaMMy	Hidden Markov modeling
I_A	Emission intensity of an acceptor molecule
I_D	Emission intensity of a donor molecule
PEG	Polyethylene glycol
sm	Single molecule
TIR	Total internal reflection
TMR	Tetramethylrhodamine
Trolox	6-hydroxy-2,5,7,8-tetramethylchromane-2-carboxylic acid
T50	Solution containing 10 mM Tris-HCl (pH 8.0) and 50 mM NaCl

2005), proteins, and large macromolecular complexes (Ha 2001a, 2004; Myong et al. 2006). A variant of smFRET based on total internal reflection (TIR) microscopy is the main focus here. (See Table 2-1 for a summary of abbreviations and acronyms used in this chapter.)

FRET is a spectroscopic technique for measuring distances in the 30–80 Å range (see also Chapter 5). Excitation energy of a donor molecule is transferred to an acceptor via interaction between two induced dipoles (Förster 1948). As shown in Figure 2-1a, the efficiency of energy transfer, E, is given by

$$E = \frac{1}{1 + (R/R_0)^6}$$

where R is the distance between donor and acceptor and R_0 is the characteristic distance at which 50% of the energy is transferred (Clegg 1992). R_0 is ~60 Å for a classical smFRET pair (Cy3 and Cy5) (Murphy et al. 2004). A sizeable change in E is observed when the distance between donor and acceptor molecules changes over several angstroms and nanometers. Therefore, a structural

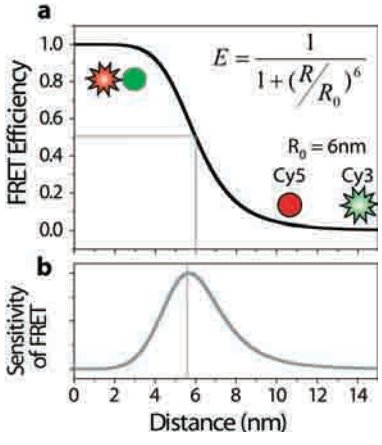

FIGURE 2-1. FRET. (*a*) Distance dependence of FRET efficiency. Cy3 (donor, *green circle*) transfers half of its energy to Cy5 (acceptor, *red circle*) when they are separated by R_0 (6 nm). (*b*) The change of FRET is the most prominent around R_0.

change of a biological molecule or a relative motion between two interacting molecules can be detected via the change in FRET (Selvin 2000).

BOX 1. CALCULATING R_0

R_0 is calculated as follows:

$$R_0^6 = \frac{9000(\ln 10)\Phi_D \kappa^2 J(\nu)}{128\pi^5 N_A n^4}$$

where Φ_D is the quantum yield of the donor molecule, N_A is Avogadro's number, and n is the index of refraction of the medium. κ^2 is an orientation factor, whose average is 2/3. $J(\nu)$ is the normalized spectral overlap of the donor emission $f_D(\lambda)$ and the acceptor absorption $\varepsilon_A(\lambda)$ as below,

$$J(\nu) = \frac{\int \varepsilon_A(\lambda) f_D(\lambda) \lambda^4 d\lambda}{\int f_D(\lambda) d\lambda}$$

where $\varepsilon_A(\lambda)$ is in units of $M^{-1}cm^{-1}$ and M^{-1} is 1000 cm^3/mole. Free software for calculating R_0 is available from http://www.photochemcad.com, or a Matlab program is available upon request.

In ensemble FRET measurements, it is often very difficult to synchronize the conformational changes of biological molecules and not feasible to detect the short-lived conformers (Fig. 2-2a). smFRET opens up new opportunities by probing the structural changes of individual biological molecules in real time (Fig. 2-2b). It readily determines the distribution of several conformations, not just the average of them (McKinney et al. 2003; Lee et al. 2005). This makes it possible to directly identify rarely visited and short-lived states (Nahas et al. 2004; McKinney et al. 2005). Postsynchronization during data analysis eliminates the need for synchronization during a measurement (Fig. 2-2c) (Blanchard et al. 2004). It is also possible to study heterogeneity between molecules (Zhuang et al. 2002; Okumus et al. 2004). Last, but not least, direct observation often reveals what people could not imagine or deduce based on ensemble measurements alone (Myong et al. 2005; Joo et al. 2006).

In comparison to other sm techniques such as FIONA, optical tweezers, and magnetic tweezers, smFRET is less prone to environmental noise because (1) it is inherently a ratiometric technique where we measure the ratio between the two different colors and (2) it reports on the internal

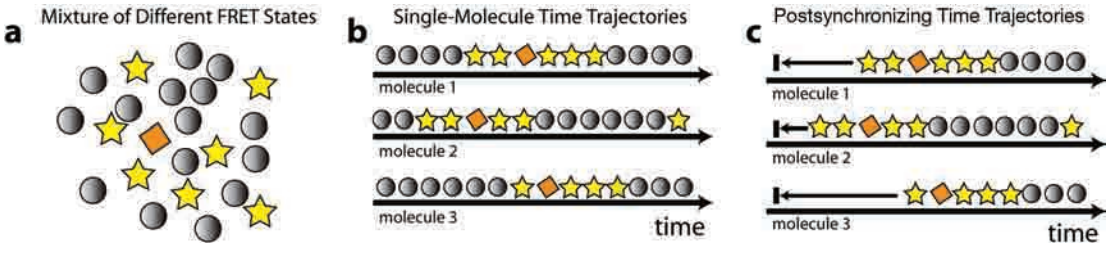

FIGURE 2-2. Single-molecule FRET study. (*a*) FRET in ensemble represents only the average value from many molecules. (*b*) The time traces of individual molecules reveal the true FRET states of different conformations in real time. (*c*) Events under study can be postsynchronized during data analysis.

movements of molecules in their center-of-mass frame. Thus, variations in the excitation and detection efficiencies between molecules are mostly tolerable. In addition, relative drift of the molecule in the lab frame is much less of an issue in comparison to the techniques that rely on determination of absolute positions in the lab frame (see below, Optical Table). In addition, it is relatively easy to acquire data from several hundred molecules compared to optical and magnetic tweezers (e.g., see below, FRET Histogram). Therefore, kinetic rates of biological events can be determined with the highest accuracy, screening out the intrinsic heterogeneity between single molecules. However, the photophysical properties of an organic dye limit its typical temporal resolution to several milliseconds (ms) (Ha 2001b).

DYE CHOICE

Ideal dyes for sm fluorescence studies should possess as many as possible of the following characteristics. They must be (1) photostable, so that they emit millions of photons before photobleaching, (2) bright (high extinction coefficient and quantum yield), (3) showing little intensity fluctuation, at least in the timescale of interesting biological events under study, (4) excitable and emitting in the visible wavelengths, (5) relatively small so that they introduce minimum perturbation to the host molecule, and (6) commercially available in a form that can be conjugated to biomolecules.

Most Favorable Dyes

Various dyes (including Alexa and Atto dyes) have been used for smFRET studies of diffusing molecules, and Cy3, Cy5, and tetramethylrhodamine (TMR) remain the dominant choices for FRET measurements of immobilized molecules because of their superior photophysical properties. Cy3 is the most stable dye we have tested, and the stability of Cy5 is greatly enhanced if the oxygen scavenger system with Trolox is used (Rasnik et al. 2006) (see Imaging Buffer). TMR is quite good and has an almost identical spectrum to Cy3 but with a lower extinction coefficient. However, it has the tendency to change its intensity between two or three different levels (C. Buranachai et al., unpubl.).

Favorite Donor and Acceptor Pair

An ideal pair of dyes for smFRET study would have (1) appreciable overlap between donor emission and acceptor absorption (Fig. 2-3a), (2) large spectral separation in donor and acceptor emission to minimize donor emission leakage into the spectral range of acceptor emission and to reduce the amount of direct excitation of the acceptor by the laser (Fig. 2-3b), and (3) a comparable emission quantum yield for donor and acceptor, which guarantees clearly anticorrelated intensity changes of donor and acceptor. Cy3 and Cy5 arguably have been the most popular donor and acceptor pair for smFRET because (1) their spectral separation is large (~100 nm) (Fig. 2-3b), (2) they are both photostable in an oxygen-free environment, (3) the quantum yields (~0.25) are comparable, and (4) they are commercially available in amino-, thiol- and other reactive forms.

Three-color FRET may require additional criteria for dye selection depending on particular applications and can be classified into the following categories according to the spectral separation between three fluorophores: (1) one-donor/two-acceptor scheme (Hohng et al. 2004a), (2) two-step FRET scheme (Clamme and Deniz 2005), and (3) two-donor/one-acceptor scheme. These categories are neither exhaustive nor mutually exclusive, and they may have pros or cons for specific applications (see below, General Scheme: Distance between Dyes).

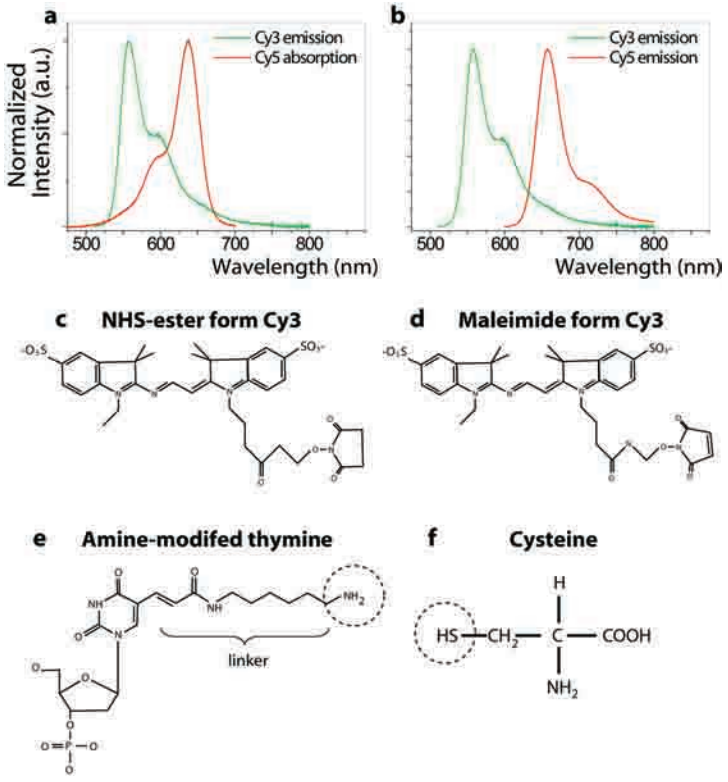

FIGURE 2-3. Fluorophore. (*a*) The emission spectrum of Cy3 (donor) overlaps with the absorption spectrum of Cy5 (acceptor). (*b*) The emission spectra of Cy3 and Cy5 are well-separated. (*c*,*d*) The molecule structures of the NHS-ester and maleimide forms of Cy3 dye, respectively. (e) Added to the base of a thymidine by a carbon linker is the amine group, which reacts with NHS-ester. (*f*) The thiol group of cysteine reacts with the maleimide.

LABELING

To carry out smFRET experiments, a single donor, an acceptor, and a biotin should be placed in specific locations in biological molecules. Mentioned below are the typical labeling methods for short oligonucleotides and cysteine-containing proteins. Note that smFRET is relatively insensitive to incomplete labeling of a host molecule. If the donor is missing, the molecule is simply not observed; if the acceptor is missing, this donor-only species shows up as a zero-FRET population.

Labeling DNA (or RNA)

Several companies offer fluorescently labeled DNA (or RNA) oligonucleotides. For example, IDT DNA (Integrated DNA Technologies) provides 5′-end labeling for a 5- to 100-nucleotide-long DNA, and 3′-end labeling for 5- to 50-nucleotide-long DNA. Labeling in the middle of the strand (internal labeling) is also offered commercially. Although a dye can be inserted using phosphoramidite chemistry during oligonucleotide synthesis, this interrupts the backbone of the oligonucleotide, which may perturb biological function. Therefore, we recommend an alternative method for internal labeling in which an oligonucleotide is synthesized with an amine-modified thymine added in a desired location (Fig. 2-3e). Reaction of the amine group with an NHS-ester form of a dye (Fig. 2-3c) followed by a simple purification procedure results in a purely labeled DNA in a day. Protocol 1, which discusses labeling DNA (or RNA), is at the end of this chapter.

Labeling Proteins

There are a number of methods for protein labeling (Schatz 1993; Heyduk 2002). Here, we briefly describe one of the popular methods. A maleimide form of a dye (Fig. 2-3d) reacts with a thiol group (-SH) with a very high specificity, and cysteine (Cys) is the only amino acid that has the thiol group among the natural amino acids (Fig. 2-3f). The reaction condition is relatively mild. Therefore, if a protein contains one Cys and if it is well-exposed on the surface, simple mixing of maleimide dyes and proteins in an appropriate solution yields good labeling. However, many proteins have more than one Cys exposed, and it is necessary to remove them via site-directed mutagenesis (Rasnik et al. 2004). Otherwise, FRET reported will represent an average value of several FRET pairs, which annuls most of the unique advantages of smFRET. If there are a large number of Cys residues present in the wild type, this labeling method is not recommended. A sample labeling protocol (Protocol 2) is at the end of the chapter. Once the labeling is successfully carried out, the functional activity of the protein should be tested for any possible artifact from the presence of dye.

CONSTRUCT DESIGN

Attaching a fluorophore in an optimal location is crucial to successful smFRET experiments. We list below several factors that should be considered in designing a construct for studying protein–DNA (or –RNA) interactions. In all cases, the presence of a dye and the physical constraint from immobilization may interfere with the activity of a protein. Therefore, one needs to cross-check with biochemical ensemble data.

General Scheme: Distance between Dyes

FRET is the most sensitive when the donor and acceptor are about R_0 apart (Fig. 2-1b). It is common to place them on the host molecule in such a way that the distance between the two dyes alternates around R_0 during the conformational change (Fig. 2-4a–c). For DNA, the internal labeling method (see above, Labeling DNA) can be used to move the fluorophore to the optimal location (Fig. 2-4a). When attaching one fluorophore to DNA and the other to a protein, or both to the protein, high-resolution structural information is crucial in determining the optimal labeling location (Fig. 2-4b).

In the three-color FRET assay (see Fig. 2-9c), because FRET occurs between all three fluorophores, the data become difficult to interpret if all three of them are brought close to each other. For example, if two different acceptors (Cy5 and Cy5.5) compete to accept energy from the donor (Cy3) (see above, Favorite Donor and Acceptor Pair) and if the two acceptors are in close proximity to each other, it will not be easy to tell whether the Cy5.5 signal is due to FRET from Cy3 or due to sequential FRET from Cy3 to Cy5 and then to Cy5.5. In such a case, it is better to design a construct in which the two acceptors are always far from each other in comparison to their R_0 (Fig. 2-4d).

DNA with Both Donor and Acceptor

In an experiment with an unlabeled protein, DNA with both donor and acceptor molecules is immobilized. Since it is impractical, in terms of yield and cost, to have all three modifications (biotin, donor, and acceptor) in one single-stranded DNA, the modifications are often added to separate DNA strands that are annealed later. For example, if a ssDNA is required, it is common to use a partial dsDNA instead (Fig. 2-4a) (Lee et al. 2005; Myong et al. 2005; Joo et al. 2006).

Proteins can change the photophysical properties of a fluorophore. For example, we have observed that the fluorescence of DNA-conjugated Cy3 increases when a protein binds nearby.

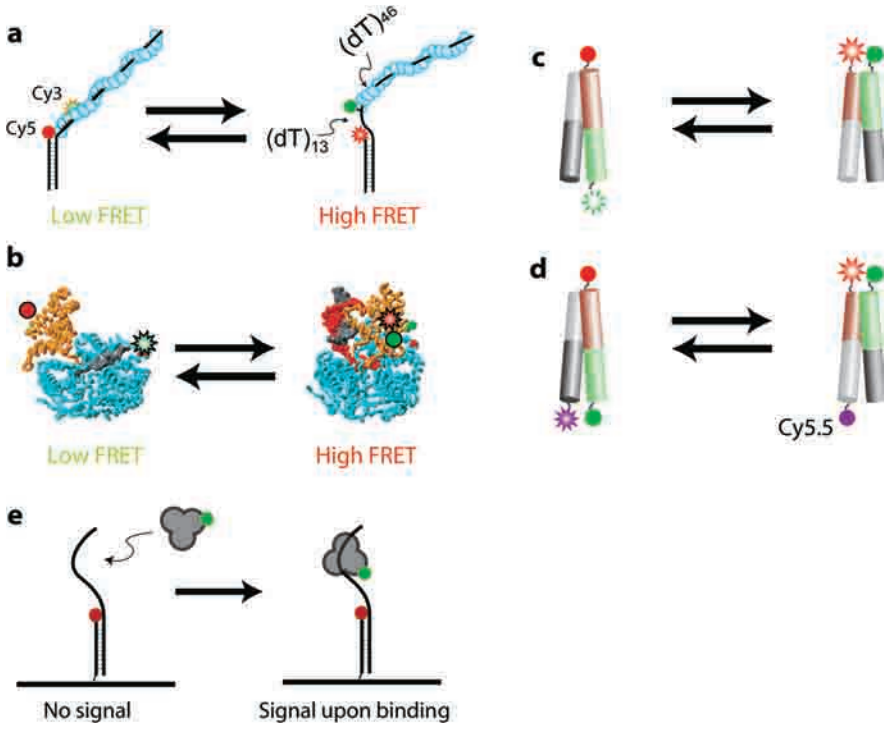

FIGURE 2-4. Sample labeling. (*a*) Cy3 and Cy5 are placed in such a way that the distance between them becomes farther than R_0 (*left*) and shorter than R_0 (*right*) in two conformations (Joo et al. 2006). (*b*) The locations of two dyes are chosen based on the X-ray crystal structures of the two conformations. Therefore, they are differentiated by two distinct FRET states (Myong et al. 2005). (*c*,*d*) The two different conformations of a four-way (Holliday) junction are visualized by two different FRET states via (*c*) a conventional two-color scheme and (*d*) a three-color scheme. In the three-color scheme, Cy5 and Cy5.5 are always well separated in both conformations; therefore, FRET between them is negligible (Hohng et al. 2004a). (*e*) When a DNA molecule is immobilized with an acceptor molecule, the signal appears only when a donor-labeled molecule binds to the DNA.

This does not present much difficulty in data interpretation because of the cancellation of the contribution to the commonly used approximation for FRET efficiency (Joo et al. 2006).

Some general design rules for labeling site selection are (1) if the protein recognizes a certain chemical feature of DNA, the fluorophore should be placed elsewhere, (2) for internal labeling, keep the backbone continuity of DNA (see above, DNA Labeling), and (3) in the DNA, the part that interacts with a protein may be placed away from the glass surface to avoid potential physical constraints.

Labeled Protein

In studying the interaction between a surface-immobilized DNA and a protein in solution, both of which are labeled, it is advantageous to attach a donor to the protein and an acceptor to the DNA because the moment of protein binding to the DNA can be unambiguously identified as a sudden increase in fluorescence signal (Fig. 2-4e; also see Fig. 2-7d). If, instead, the protein is labeled with the acceptor and DNA with the donor, initial binding to a low-FRET state may not be detected. Also, any additional FRET change that occurs after protein binding cannot be easily distinguished from additional protein binding if the acceptor is on the protein. If the fluorescent species in solution is too high in concentration, background fluorescence can overwhelm the single-molecule signal. This can occur if the donor concentration is higher than 2 nM and if the acceptor concentration is higher than 20 nM. If affinity is low and a higher concentration is needed, it is better to use unlabeled proteins and measure their activities on DNA via the changes in DNA conformations (Joo et al. 2006).

SURFACE PREPARATION

To study the conformational changes of individual molecules over extended time periods, molecules must be localized in space. This is often achieved by surface immobilization (Rasnik et al. 2005). An ideal surface would allow specific immobilization of DNA, RNA, or proteins while rejecting nonspecific adsorption. For nucleic acid studies, we prefer to use a glass (or quartz) slide coated with biotinylated BSA and neutravidin (or streptavidin) because of this system's simplicity (Fig. 2-5a). We can immobilize DNA (or RNA) with high specificity (>500:1, compared to control experiments that exclude biotin or neutravidin) and are able to reproduce their bulk solution activities faithfully (McKinney et al. 2003, 2005; Tan et al. 2003; Hohng et al. 2004b; Murphy et al. 2004; Nahas et al. 2004; Lee et al. 2005). This is likely because all three surface constituents (BSA, neutravidin, and glass) are negatively charged at neutral pH, repelling nucleic acids.

For studies involving proteins, a BSA-coated surface is too adhesive. Therefore, we developed a polyethylene glycol (PEG)-coated surface that reduces the protein adsorption to an undetectable level (Fig. 2-5b). Surface passivation using PEG, first introduced for single-molecule studies in 2002 (Ha et al. 2002), has now been adopted successfully by several other groups. If a dense layer of PEG is formed on a glass surface, it forms a polymer brush that prevents protein adsorption to the underlying surface. We incorporate a small fraction of PEG polymers that are end-modified by biotin to immobilize neutravidin, which further immobilizes biotinylated macromolecules. Proteins interact specifically with DNA immobilized to the PEG-coated surface, and their bulk solution activities are well reproduced in all systems we have tested (Ha et al. 2002; Rasnik et al. 2004; Myong et al. 2005; Joo et al. 2006). We have also developed a vesicle encapsulation technique that can measure conformational dynamics of biomolecules free of surface tethering (Okumus et al. 2004; Cisse et al. 2007). See Protocol 3 for descriptions of tethering single molecules on BSA- and PEG-coated surfaces.

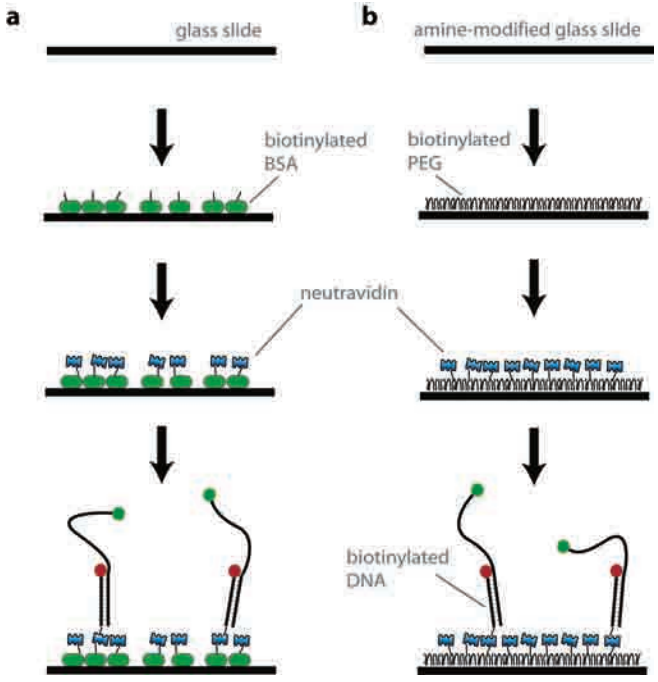

FIGURE 2-5. Sample immobilization. (*a*) On the naked glass surface, biotinylated BSA is deposited and then neutravidin is conjugated with biotinylated BSA. A biotinylated specimen (here DNA) is then immobilized via biotin–neutravidin binding. (*b*) On the amine-modified glass surface, the NHS-ester form of PEG is covalently conjugated. Neutravidin specifically binds to a fraction of PEG molecules that have biotin at their ends.

DATA ACQUISITION

Imaging Single Molecules

There are always some fluorescent impurities on the surface, and without experience in sm imaging, it is often difficult to distinguish the molecules of interest from impurities. Protocol 4 addresses this issue.

Imaging Buffer

The photostability of Cy dyes (especially Cy5 and Cy5.5) is greatly improved by the oxygen scavenger system and by reducing agents (Rasnik et al. 2006). The preparation of the imaging buffer is detailed in Protocol 4. The oxygen scavenger system consists of 0.4% w/v β-D-glucose or 0.8% w/v D-glucose, 1 mg/ml (165 U/ml) glucose oxidase, and 0.04 mg/ml (2170 U/ml) catalase. The coupled reactions are:

$$\beta\text{-D-glucose} + O_2 + H_2O \xrightarrow{\text{glucose oxidase}} \text{gluconic acid} + H_2O_2$$

$$H_2O_2 \xrightarrow{\text{catalase}} H_2O + 1/2\ O_2 \quad \text{(Benesch and Benesch 1953)}$$

Triplet-state quenchers or reducing agents can further improve the photostability of Cy dyes. Previously, we used 140 mM β-mercapto ethanol (βME) (Zhuang et al. 2000), but we have recently found that Trolox is more effective in quenching the triplet state and at much lower concentrations (1–2 mM) than βME (Rasnik et al. 2006).

Data Acquisition Programs

Fluorescence signal is recorded in real time using home-written Visual C++ software (Microsoft) with the highest time resolution of 30 ms or shorter (see below, Detector Choice) (program available upon request). The software obtains each frame of the movie from the camera and writes it to the hard drive as a single large file that contains all the frames where each pixel is encoded as a single byte (8 bit). Typically, a 1-minute movie at 100 msec per frame occupies about 150 MBytes of hard drive space. sm traces are extracted from the recorded movie file using scripts written in IDL (Research Systems) (program available upon request). Because of aberrations and imperfect alignments of the optical system, the donor and acceptor images cannot be simply overlaid via a mere offset. By using IDL scripts and a calibration image obtained using fluorescence beads (see Protocol 6), we can determine a polynomial map between the two channels, which includes rescaling, rotation, and shear distortion.

POSTPROCESSING OF TIME TRACES

Basic data analysis on the sm traces is carried out with Origin and software written in Matlab (available upon request).

Calculating FRET Efficiency

We calculate the apparent FRET efficiency by

$$E_{app} = \frac{I_A}{(I_D + I_A)}$$

where I_D and I_A are the sensitized emission intensity of the donor and acceptor, respectively. What we actually measure are the raw intensities of the donor and acceptor channels, I_D^0 and I_A^0. We then

need to correct for the leakage of donor signal to the acceptor channel, which is typically between 10% and 15% of the donor signal and can be determined from a donor-only molecule; we subtract a fixed fraction α of I_D^0 from I_A^0 such that the corrected acceptor signal becomes zero (and $E_{app} = 0$). Whether we add back the subtracted acceptor signal to the donor signal has not been consistent for different publications, although we tend not to add it back:

$$E_{app} = \frac{(I_A^0 - \alpha \times I_D^0)}{(I_D^0 + I_A^0 - \alpha \times I_D^0)}$$

An additional correction may also be applied, because there can be a finite amount of bleed-through of the acceptor signal into the donor channel, depending on the optical configuration.

The absolute FRET value can be estimated from the above corrected FRET by using a correction factor (Ha et al. 1999). FRET efficiency is given by

$$E = \frac{I_A}{(I_D + \gamma \times I_A)}$$

where γ is a parameter representing relative detection efficiencies and quantum yields of the two dyes, and can be determined from photobleaching events. Our data using Cy3 and Cy5 show that $\gamma \approx 1$. Thus, $E \equiv I_A / (I_A + I_D)$ is an excellent approximation for FRET efficiency.

Typical Traces and General Analysis Methods

If smFRET data display temporal fluctuations (Fig. 2-6), the data are further analyzed by dwell-time, cross correlation, or hidden Markov modeling (depending on the type of fluctuation), as described below. Note that a unique signature of a sm trace is the single-step photobleaching.

Dwell-Time Analysis

If there are only two FRET states, A and B, that are interconverting (Fig. 2-6a,b), we measure the dwell-times of individual states from which we can estimate kinetic rates of the transitions. After selecting the individual transitions either manually or via automated threshold analysis, we fit the dwell-time histogram of each state to obtain the lifetimes (τ_A and τ_B, Fig. 2-6c) and the corresponding transition rates, $k_{A\to B}$ and $k_{B\to A}$.

Cross (or Auto) Correlation Analysis

When the timescale of the fluctuation between the two states is too fast for a reliable dwell-time analysis (Fig. 2-6d), we can resort to correlation analysis. For example, cross correlation can tell us whether the donor and acceptor intensities are fluctuating in an anticorrelated manner, and, if so, what the timescale is:

$$CC(\tau) = \int I_D(t) I_A(t - \tau) dt$$

Ideally, one would see a curve that starts from a negative value and decays to zero. Then, by fitting the curve using a single-exponential curve,

$$-Ae^{-(k_{A\to B} + k_{B\to A})\tau}$$

one can obtain the sum of the two rates (Fig. 2-6e, right). If the FRET efficiency histogram is clean enough to yield a measure of the relative populations of the two species (Fig. 2-6e, left), that is, $k_{A\to B}/k_{B\to A}$, in combination we can determine both $k_{A\to B}$ and $k_{B\to A}$ (Tan et al. 2003; Joo et al. 2004).

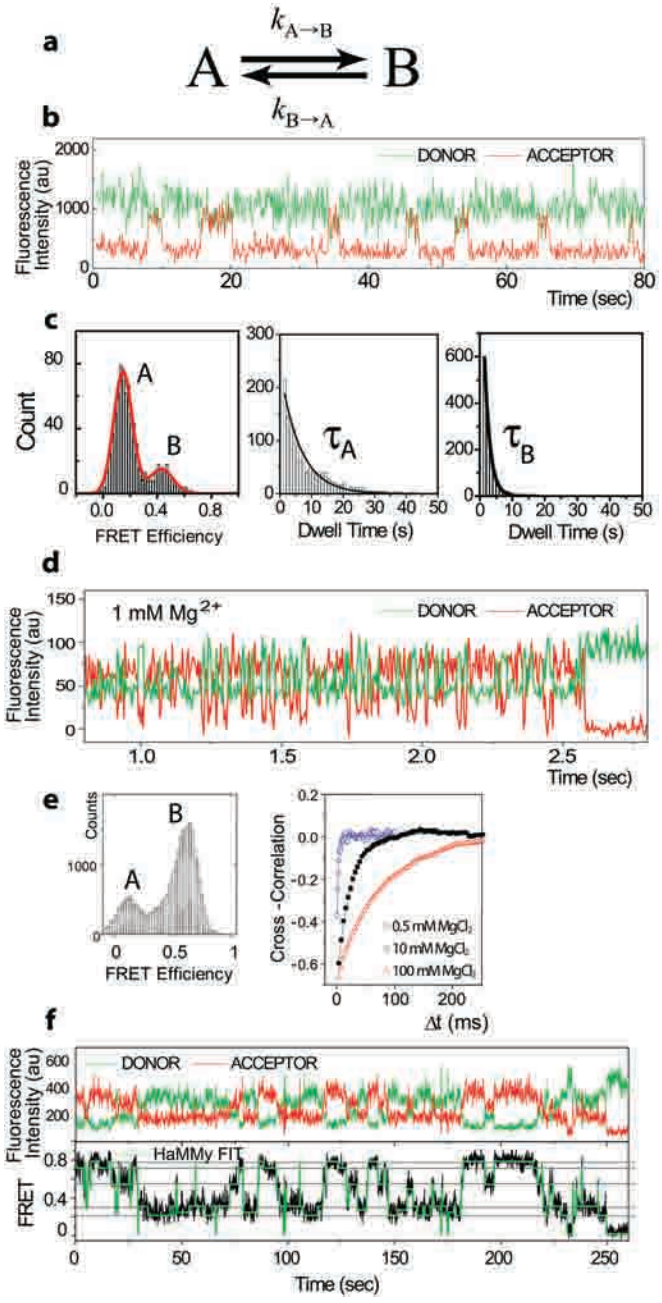

FIGURE 2-6. Conformational dynamics in equilibrium. (*a*) The scheme of two-state dynamics whose examples are in *b*–*e* below. (*b*) A sm-time trace shows a two-state fluctuation between high and low FRET states. The donor signal (*green*) is anticorrelated with the acceptor signal (*red*) (Hohng et al. 2004a). (*c*) On the *left* is a FRET histogram from the data in *b*, and the other two panels show the dwell-time distribution of low and high FRET states, respectively. τ_A is equal to $1/k_{A\to B}$ and τ_B to $1/k_{B\to A}$. (*d*) When the fluctuation between two states becomes too fast, it is hard to use dwell-time analysis. A cross-correlation method is an alternative (Joo et al. 2004). (*e*) On the *left* is a FRET histogram from the data in *d*, and on the *right* the cross correlation between the donor and acceptor time traces in different salt concentrations. (*f*) When there are more than two states observed (here, six including photoblinking of acceptor), an advanced algorithm such as HaMMy is required for reliable data analysis. The fit (*green line*) over the FRET trace is from HaMMy analysis (Joo et al. 2006).

Hidden Markov Modeling

If there are more than two states (Fig. 2-6f), more complex and time-consuming procedures are required when using dwell-time and correlation analysis. In such cases, unbiased analysis tools, such as hidden Markov modeling (HaMMy) are recommended. HaMMy (available for download at http://bio.physics.uiuc.edu/HaMMy.html) is more reliable, reproducible, and less susceptible to human bias than traditional thresholding algorithms (McKinney et al. 2006). Once idealized trajectories are generated using HaMMy, the existence of discrete FRET states and how they are interconnected can be evaluated by using a transition density plot, yet another layer of data reduction which is also available from the above link.

Not all the data are suitable for HaMMy. A good rule of thumb is: If you can almost see where the discrete states are by eye but cannot begin to do quantitative analysis, then try HaMMy. The data need to have multiple transitions within each trace. Ideally, all states should be visited multiple times for the best result. The lifetime of each state should be at least the time resolution of the data, and if there are multiple states with identical FRET values, the Markovian nature of the algorithm cannot work, at least not reliably. In summary, HaMMy is powerful but it does not do magic!

Other Types of Traces

Solution Exchange during Recording

When the solution condition changes via flow during a measurement (see Protocol 3), the response of a molecule is visualized in real time (Fig. 2-7a).

Disappearance of Signal

When FRET approaches zero, one must distinguish whether this is because of photobleaching of the acceptor or because of transition to a true low-FRET state. Direct excitation of the acceptor is the most straightforward method (Fig. 2-7b). If the total signal is lost after reaction, there is no direct method of identifying whether it is a result of the reaction or a result of photobleaching of donor molecules (Fig. 2-7c). As a control, one can measure the photobleaching timescale of the donor under the same condition except that the biochemical reaction of interest is disabled. In addition, the same reaction can be performed at multiple laser excitation intensities to check whether the reaction time depends on the excitation power. If so, it is likely that much of the fluorescence loss is due to photobleaching.

Appearance of Signal

When a dye-labeled molecule approaches from a solution, its binding to the immobilized molecule results in the digital appearance of fluorescence signal. As explained earlier (see above, Labeled Protein), if the approaching molecule is labeled with a donor (instead of an acceptor), the time when the molecule binds is easily identified (Fig. 2-7d).

FRET Histogram

FRET histograms are built by taking the average FRET efficiency of the first ten frames for each molecule, typically out of more than 1000 molecules from multiple imaging areas. When a single peak represents only one FRET state, it is typically less than 0.1 full-width-half-maximum wide (e.g., Fig. 2-6c, left). Statistical and instrumental noise inhibits further resolution of the peak.

Because the FRET histogram is built from a great number of molecules, it provides statistics in the quickest and most unbiased way. For example, as shown in Figure 2-8, different concentrations of KCl change the distribution of the FRET histogram very clearly. After this type of quick survey over several different solution conditions, we move on to a more rigorous and time-consuming step—to record smFRET traces and to carefully analyze them one by one.

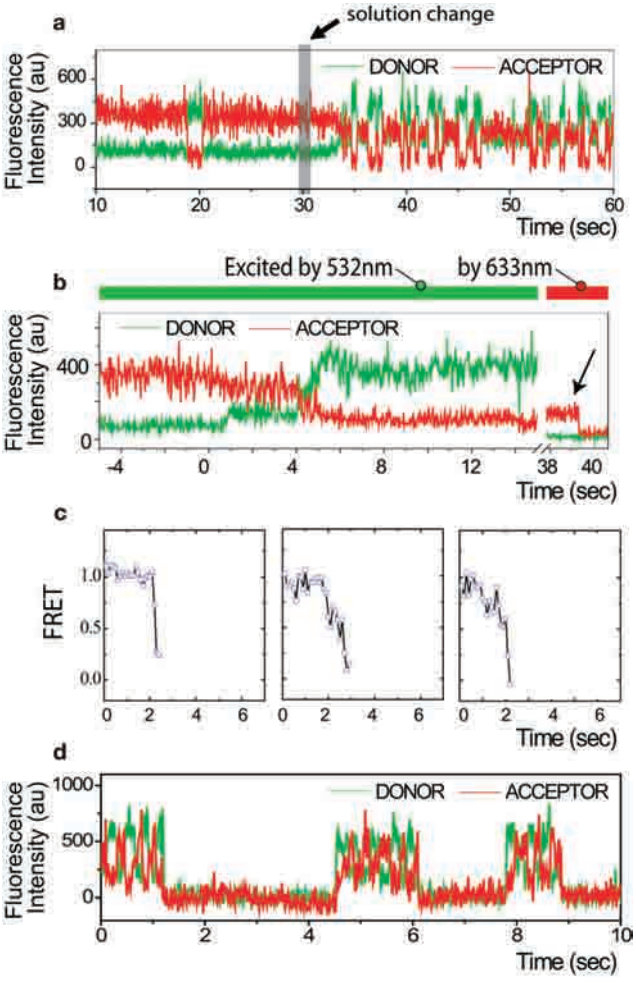

FIGURE 2-7. Non-equilibrium conformational dynamics. (*a*) Upon solution exchange at $t \sim 30$ sec, a change in conformation occurs (Buranachai et al. 2006). (*b*) Upon solution exchange at $t \sim 0$ sec, FRET drops to near zero. The activity of the acceptor is confirmed by directly exciting acceptor molecules at $t > 38$ sec (*arrow*) (Joo et al. 2006). (*c*) When a protein that unwinds double-stranded DNA interacts with DNA immobilized on a surface, not only does FRET change, but the total signal soon disappears (Ha et al. 2002). (*d*) If acceptor-labeled DNA is immobilized on a surface, fluorescence signal is observed only when a donor-labeled protein interacts with the DNA (Myong et al. 2005).

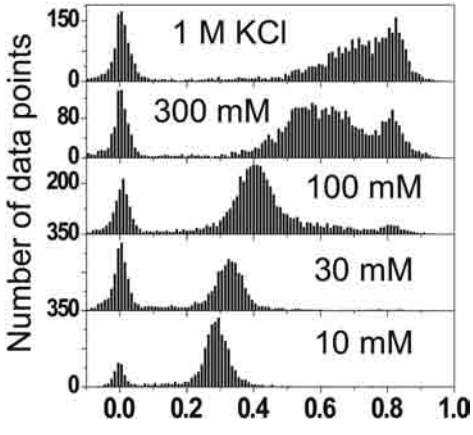

FIGURE 2-8. FRET histogram. Different conformations of G-quadruplex DNA in different potassium concentrations are revealed by the change in distribution of FRET histograms. The peak at $E = 0$ corresponds to the donor-only population (Lee et al. 2005).

The inactive acceptor molecules contribute to the peak at $E_{app} = 0$. In principle, this FRET value cannot be smaller than 0. In practice, I_A is very small for FRET approaching 0, and noise around the background level makes I_A negative after background subtraction, leading to calculated FRET values smaller than 0. For the same reason, FRET values larger than 1 can be obtained if it is close to 1.

DESIGN AND CONSTRUCTION OF SETUP

Our setup is built around a commercial inverted microscope (Olympus). Commercial solutions are available for TIR microscopy, but we prefer to build our own because of the lower cost and maximum flexibility. The custom-made add-ons can be divided into excitation and emission. In brief, Cy3 molecules are excited by an Nd:YAG laser (532 nm) via TIR. The fluorescence signal from Cy3 and Cy5 that is collected by an oil-immersion (objective-type) or by a water-immersion (prism-type) objective lens goes through a long-pass filter to block out laser scattering. The donor and acceptor signals are separated by a dichroic mirror and are detected by a charge-coupled device (CCD) camera with up to 1 ms time resolution. The observation area is about 25 μm × 50 μm. The details of how to build the setup are described below. The emission optics for a three-color setup are shown in Figure 2-9c.

Detector Choice

Signal amplification is necessary to suppress the readout noise in high-speed CCD imaging. The new generation of electron multiplying CCD cameras (iXon, Andor Technology) use on-chip multiplication that adds minimal noise (at worst, noise increases by ~50% compared to the shot noise limit) while eliminating readout noise through amplification. The back-thinned version achieves more than 80–90% quantum yield over the entire visible light range, comparable to the best-performing silicon avalanche photodiodes (APD). The time resolution is currently 30 msec for 512 × 512 pixels without any binning and 16 msec for 512 × 256 pixels. With 2 × 2 binning, we can obtain 8-msec time resolution. The smaller EMCCD (iXon, Andor Technology), 128 × 128 pixels, can achieve 2-msec time resolution without binning, and 1 msec with binning. We set the temperature of the CCD chip at –75°C and obtain sm traces with a gain of 230.

The still remaining advantages of confocal detection using avalanche photodiodes are (1) better instrumental time resolution (although ultimately the real-time resolution is limited by photophysics, which might have been improved with the adoption of Trolox [see above, Imaging Buffer]) and (2) the possibility of doing lifetime measurements (Laurence et al. 2005). For a description of the smFRET using confocal microscopy, see Chapter 5.

Optical Table

The laser table or optical table (e.g., RPR Reliance Series with RL-2000 Series LabLegs, Newport) is typically used, but a 1″-thick breadboard (Newport) with uniformly spaced 1/4″-20 threaded holes mounted on a regular laboratory bench or desk is stable enough for TIR FRET.

Objective-type TIR Microscopy

Of the two options, prism- and objective-type TIR, we now prefer objective-type TIR because of its ease of use. In the past, objective-type TIR provided high background from the acceptor channel and was therefore deemed inadequate for FRET. However, the new generation of 1.4 numerical aperture (NA) oil-immersion objectives (e.g., UPlanSApo from Olympus) has largely solved this problem. There is still slightly higher background than in prism-type TIR, as can be judged by a visual scan, but the actual signal-to-noise ratio of single-molecule data is indistinguishable. Careful alignment procedures, as detailed in Protocol 5, still allow a large excitation field of view

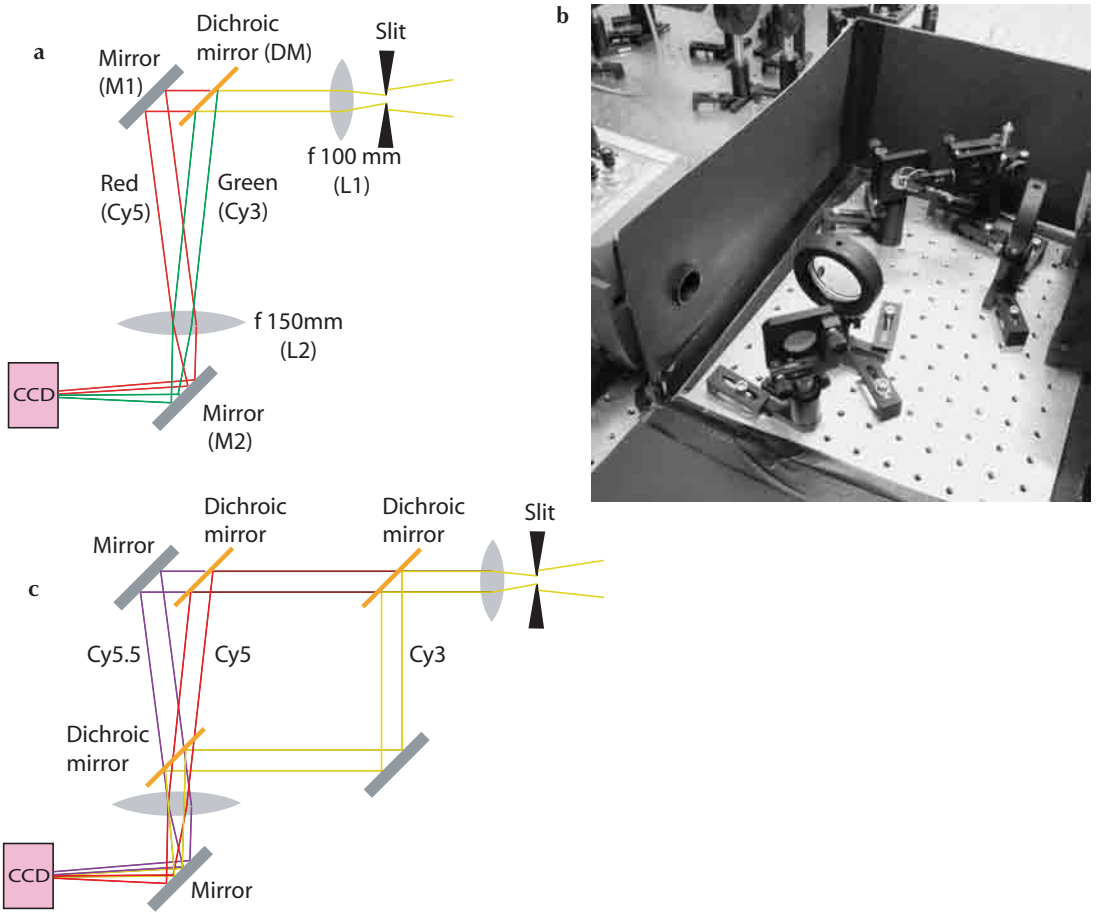

FIGURE 2-9. Emission optics. (*a*) In two-color emission optics, the collimated beam goes through a dichroic mirror where the donor signal is reflected. After passing through a lens (M2), the donor and acceptor images are projected onto one-half of the CCD screen each. (*b*) Photo of the two-color setup (bird's eye view). (*c*) In the three-color setup, the donor signal is separated first, then the other two colors are later split in the same way as in *a*. The donor signal is then combined with the other two by another dichroic mirror and projected onto the CCD screen.

so there is really no need for higher NA objectives such as 1.45 NA (with known spherical and chromatic aberration problems) or 1.65 NA (requiring a special glass coverslip and immersion oil with a higher refractive index). Protocol 6 provides the details on building detection optics shown in Figure 2-9.

Prism-type TIR Microscopy

Prism-type TIR has been a major imaging tool for smFRET since it was first introduced (see Protocol 7). The limitations of the setup are (1) it is often difficult to identify the excitation area on a sample surface, (2) the top side of the chamber is covered by a prism, which is inconvenient, and (3) it requires relatively expensive and brittle quartz slides. All these limitations are overcome by objective-type TIR. However, it is only with prism-type TIR that a flow technique (see Protocol 3) can be practiced reliably. The introduction of flow results in the bowing of the imaging surface, which is a coverslip in objective-type TIR, and this leads to defocusing during data acquisition.

Protocol 1

Labeling DNA (or RNA)

This protocol for labeling nucleic acids is optimized for 5 nmole of DNA that has an amine-modified thymine in its sequence. It is a simplified version of a protocol from Invitrogen.

MATERIALS

CAUTION: See Appendix for appropriate handling of materials marked with <!>.

Reagents

Dimethyl sulfoxide (DMSO; Fisher Scientific) <!>
DNA sample
Dyes (monofunctional NHS ester form)
  Alexa and other dyes (Invitrogen)
  Cy3 (GE Healthcare [PA13101])
  Cy5 (GE Healthcare [PA15101])
  Cy5.5 (GE Healthcare [PA15601])
Ethanol (cold)
HCl (12.1 M) <!>
Sodium chloride (NaCl, 3 M; Fisher Scientific)
Sodium tetraborate (Fisher Scientific)

Equipment

Microcentrifuge tubes
Spectrophotometer

METHODS

1. Dissolve the DNA in MilliQ H_2O (18.5 MΩ) to a final concentration of 1 mM.

   Tris or compounds carrying amine groups interfere with the labeling reaction. Remove them by ethanol precipitation of the oligonucleotide prior to labeling.

2. Prepare fresh labeling buffer (0.1 M) by dissolving 380 mg of sodium tetraborate in 10 ml of MilliQ H_2O. Add 65 µl of 12.1 M HCl or equivalent to bring the pH to 8.5.

   High pH enhances the acylation rate; however, it also increases the hydrolysis of the esters.

3. Dissolve 1 mg of dye in 56 µl of DMSO (~20 mM).

   Store excess dye solution in aliquots at –20°C. It is not highly stable in solution.

4. Mix the following components in a microcentrifuge tube:

   5 µl of dye in DMSO

   25 µl of 0.1 M labeling buffer

   5 µl of 1 mM DNA or equivalent (5 nmole total)

   This composition results in about 20 dye molecules for each reactive amine group. If there is not enough DNA available, linearly rescale the amount of the dye and the labeling buffer.

5. Incubate the mixture for 6 hours at room temperature and/or overnight at 4°C with gentle mixing in the dark.

6. Add 87.5 µl of cold ethanol and 3.5 µl of 3 M NaCl to the mixture and keep it at –20°C for 30 minutes. Centrifuge at 12,000*g* for 30 minutes at 4°C. Remove the supernatant carefully and rinse the pellet with cold ethanol several times very gently. Dry the DNA pellet to evaporate the ethanol. Dissolve the pellet in an appropriate solution.

7. Check the labeling efficiency by comparing the absorption spectra of the DNA (260 nm) and the conjugated dye. Typically, it is close to 100%. If not, run an additional purification such as denaturing PAGE to separate the labeled from the unlabeled DNA, or repeat Step 6.

Protocol 2

Labeling Proteins

This protocol is based on the labeling procedure of *E. coli* Rep helicase (Rasnick et al. 2004). A different assay (e.g., different chemical conditions) may be required for other proteins.

MATERIALS

CAUTION: See Appendix for appropriate handling of materials marked with<!>.

Reagents

Buffer A (50 mM Tris-HCl [pH 7.67], 150–500 mM NaCl, 10–25% glycerol; degas by 20 minutes of sonication)
Dimethyl sulfoxide (DMSO; Fisher Scientific) <!>
Dyes (monofunctional maleimide form)
  Alexa and other dyes (Invitrogen)
  Cy3 (GE Healthcare [PA13131])
  Cy5 (GE Healthcare [PA15131])
  Cy5.5 (GE Healthcare [PA15631])
His-tagged protein (~10 ml of 20 μM or equivalent)
Imidazole (1 M [pH 8.0]; high purity; Sigma-Aldrich) <!>
Ni^{2+}-NTA agarose beads (Qiagen) <!>
Nitrogen <!>
Tris-(2-carboxyethyl) phosphine hydrochloride (TCEP; Invitrogen) <!>

Equipment

Chromatography columns (Poly-Prep; Bio-Rad)
Microcentrifuge tubes
Spectrophotometer

METHODS

1. Equilibrate the Ni^{2+}-NTA beads with Buffer A. Mix the His-tagged protein (~10 ml of 20 μM or equivalent) with 1.5 ml of the Ni^{2+}-NTA beads and place the mixture onto a chromatography column. Carry out all the procedures at 4°C unless otherwise specified.
2. Flush the column with more than 4 column volumes (CV) of Buffer A. Next, flush with 1 CV of 0.1–0.2 mM TCEP dissolved in Buffer A and incubate for 10 minutes at room temperature. Then, flush with another 20 CV of Buffer A.
3. Add a small amount (<1 ml) of Buffer A and transfer the sample to 1.5-ml tubes (500 μl of sample per tube).

4. Degas the sample by gently blowing with nitrogen for 1 minute (to achieve the highest labeling efficiency). Close the tubes immediately and keep the tubes at room temperature for 10 minutes.
5. Dissolve 1 mg of dye in 56 µl of DMSO (~20 mM). Store excess dye solution in aliquots at –20°C. It is not highly stable in solution.
6. Add dye to the sample to a final ratio of about 1:10 (protein:dye molecules). Repeat Step 4 and incubate the mixture overnight at 4°C with gentle mixing in the dark.
7. Load the sample onto a chromatography column and flush with 10 CV or more of Buffer A until all the unconjugated dye molecules are flushed out of the column.
8. Elute the labeled protein by adding 0.2 M imidazole in Buffer A to the column.
9. Check the labeling efficiency by comparing the absorption spectra of the protein (280 nm) and the conjugated dye molecule.

   Use of low-quality imidazole results in high absorption at 280 nm, which inhibits the proper measurement of the protein concentration.

Protocol 3

Preparing Sample Chambers

This protocol describes the preparation of sample chambers with either BSA- or PEG-coated slides to which single molecules can be tethered for use in FRET studies.

MATERIALS

CAUTION: See Appendix for appropriate handling of materials marked with <!>.

Reagents

Acetic acid (glacial; Fisher Scientific) (for PEG surface)
Acetone (Fisher Scientific) <!>
Alconox (Alconox) <!> (for PEG surface)
Amino silane (N-(2-aminoethyl)-3-aminopropyltrimethoxysilane; United Chemical Technologies) <!> (for PEG surface)
Biotin-PEG (MW 5000; Biotin-PEG-SC; hydrolysis half-life >20 minutes; Laysan Bio) (for PEG surface)
Biotinylated bovine serum albumin (BSA; Sigma-Aldrich)
Biotinylated DNA (50 pM in an appropriate buffer, usually buffer T50 containing 0.1 mg/ml BSA)
BSA (New England Biolabs)
Buffer T50 (10 mM Tris-HCl [pH8.0], 50 mM NaCl)
Cy3-labeled DNA (1 nM in buffer T50)
Cy3-labeled protein (1 nM)
Methanol (Fisher Scientific) <!> (for PEG surface)
mPEG (MW 5000; mPEG-SC; hydrolysis half-life > 20 minutes; Laysan Bio) (for PEG surface) <!>
Neutravidin (ImmunoPure NeutrAvidin Protein; Pierce)
Potassium hydroxide (KOH; 1 M in MilliQ H_2O; Fisher Scientific) <!>
Sodium bicarbonate (Fisher Scientific) (for PEG surface)
Streptavidin (Invitrogen)

Equipment

Automated pump (PHD 22/2000 series syringe pump; Harvard Apparatus) (optional; see Step 8iii)
Coverslips (24 x 40 mm, No.1½, rectangular; VWR)
Diamond drill bits (3/4 mm; Kingsley North or UKAM Industrial Superhard Tools)
Double-sided tape (~100-µm thick; 3M)
Epoxy (5 minute; Devcon)
Flask (Pyrex; Fisher Scientific) (for PEG surface)
Glass staining dishes (Fisher Scientific)
Needle (26-gauge, 3/8″; Becton Dickinson)
Pipette tips (200 µl)
Propane torch (Bernzomatic) <!>
Slides (glass microscope, 1″ x 3″, 1 mm thick; Gold Seal)
Slides (quartz microscope, 1″ x 3″, 1 mm thick; G. Finkenbeiner) (for prism-type TIR)

Sonicator (Bransonic tabletop ultrasonic cleaner; Branson)
Syringe (1 ml; Becton Dickinson)
Tube (28-gauge, PTFE tubing; Hamilton)

METHODS

Preparing and Cleaning Slides and Coverslips

1. Drill two 0.75-mm-diameter holes into a glass slide to form the inlet and outlet of the chamber that will be made. Further bore one of the holes (~0.8 mm) to allow a tube to be inserted. Solutions will ultimately be injected through these holes.
2. Sonicate the slides in a glass staining dish for 20 minutes in 10% alconox, 5 minutes in tap H_2O, 15 minutes in acetone, and 20 minutes in 1 M KOH. Sonicate the coverslips in another glass staining dish for 20 minutes in 1 M KOH.
3. Rinse the slides and coverslips with deionized MilliQ H_2O (18.5 MΩ).
4. Burn the surface to be imaged using a propane torch to remove any fluorescent organic molecules. Burn a quartz slide for the prism-type TIR for half a minute. Burn a coverslip for the objective-type TIR for just a few seconds to prevent glass deformation.

   To prepare a BSA-coated surface, continue with Sample Chamber Preparation (Steps 5–6) and Solution Injection (Steps 7–9), and then follow Steps 10–13. To prepare a PEG-coated surface, go to Steps 14–20.

Sample Chamber Preparation

Assemble the chamber immediately before each experiment.

5. Attach two pieces of double-sided tape (~100-µm thick) to a cleaned slide such that there is about a 5-mm gap between the tapes to be used as spacer. Put a cleaned coverslip over the slide to form a 10–20-µl volume sample chamber (Fig. 2-10a). When assembling a PEG-coated chamber, be sure to place the PEG-coated sides facing inside the chamber.
6. Seal the remaining boundaries between the sample chamber and the outside using 5-minute epoxy.

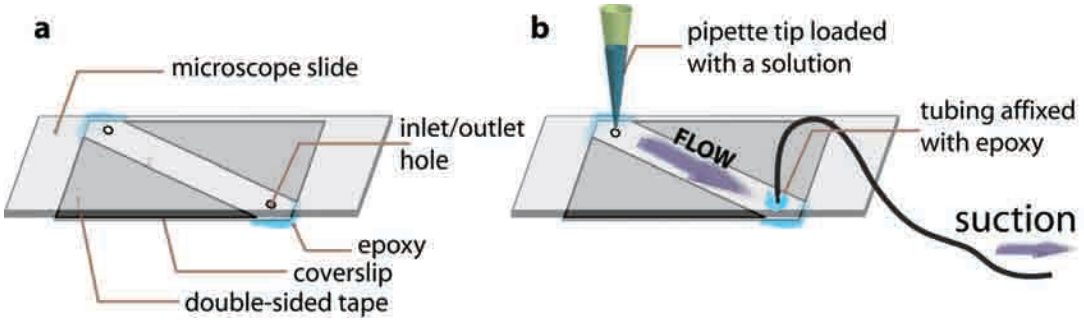

FIGURE 2-10. Sample chamber. (*a*) A sample chamber is made by putting a microscope slide and a coverslip together with double-sided tape and sealing with epoxy. The holes on the slide are used for the inlet and outlet of solution exchange. (*b*) A syringe is connected to the chamber through tubing, and a pipette tip that contains a solution is snugly plugged into an inlet hole. When the syringe is pulled, the solution is introduced into a chamber.

Solution Injection

7. Inject solutions as needed through one of the holes which has been drilled, using a 200-µl pipette tip.

   This system has the advantage that many solution conditions can be explored by flowing different solutions through the same sample chamber. Small holes minimize evaporation during prolonged measurements and reduce oxygen uptake by the solution, thereby reducing photobleaching effects and solution acidification.

8. When the solution needs to be changed during data acquisition (Fig. 2-7a), use a syringe system as follows (Fig. 2-10b):

   i. Create a flow system in an assembled chamber by attaching a 28-gauge tube to the 0.8-mm-wide hole with epoxy.

   ii. Link the tube to a 26-gauge, 3/8-inch needle, which is connected to a 1-ml syringe.

   iii. Inject the required solution into the chamber by snuggly plugging the 200-µl pipette tip containing solution to the inlet. Pull the syringe either manually or via an automated pump.

9. After use, put the chambers in tap H_2O overnight, which helps remove the double-sided tape and epoxy and thus allows slide recycling.

BSA-coated Surface

Prepare this surface just before each experiment (Fig. 2-5a).

10. Prepare a solution of 1 mg/ml biotinylated BSA in buffer T50. Flow 30 µl of this solution through the chamber. Incubate for 5 minutes.

    BSA nonspecifically adsorbs to the chamber surfaces.

11. Wash away the biotinylated BSA solution by flowing through 100 µl of buffer T50.

12. Prepare a solution of 0.2 mg/ml neutravidin or streptavidin in buffer T50. Introduce 30 µl of this solution into the chamber. Incubate for 1 minute. Wash out as in Step 11.

13. Add 30 µl of biotinylated DNA (50 pM in an appropriate buffer) to the chamber.

    This protocol allows the stepwise deposition of reagents without sample drying and typically results in a surface concentration of DNA suitable for sm imaging. Further information on DNA immobilization is found in Protocol 4, Imaging Single Molecules.

PEG-coated Surface

14. Place the cleaned coverslips and slides back into glass staining dishes in methanol.

15. Amino-modify the slides and coverslips as follows:

    i. Clean a Pyrex flask with methanol by sonicating for 5 minutes.

    ii. Mix 100 ml of methanol, 5 ml of acetic acid, and 1 ml of amino silane.

    iii. Immediately replace the methanol in the glass staining dishes with this mixture. Incubate for 20 minutes and sonicate for 1 minute in the middle of the incubation.

    iv. Replace the mixture with methanol. Store the slides and coverslips in methanol until the next step.

16. Coat the amine-modified surfaces with PEG as follows:

    i. Rinse the slides and coverslips with MilliQ H_2O. Place on a level surface.

ii. Prepare the reaction solution by dissolving 0.2 mg of biotin-PEG and 8 mg of mPEG in 64 µl of freshly made 0.1 M sodium bicarbonate (pH 8.5) for each slide. Centrifuge at 7200*g* for a minute to remove bubbles.

iii. Apply 70 µl of the reaction solution to each slide. Place a coverslip over each slide to spread the solution evenly and to prevent drying.

iv. Incubate the slide/coverslip sandwiches in a dark and humid environment overnight. Use a box which is kept humid by adding H_2O to the bottom.

v. Disassemble the sandwiches, rinse with MilliQ H_2O and store at –20°C until use. Before continuing with Steps 17–20, go to Steps 5–6 for sample chamber preparation and Steps 7–9 for solution injection.

17. After assembly, inject buffer T50 and incubate for 5 minutes. Then check the nonspecific binding of DNA by injecting 1 nM Cy3-labeled DNA in buffer T50.

18. Next, check the nonspecific binding of a protein by adding 1 nM Cy3-labeled protein.

    We use Rep helicase but any sticky protein should work fine.

    In both cases, on a good PEG-coated surface, fewer than 10–20 molecules should be visible in each 25 µm x 50 µm imaging area.

19. Once the chamber passes the quality test, fill the chamber with 30 µl of 0.2 mg/ml neutravidin solution in buffer T50. Incubate for 1 minute and wash the neutravidin out by flowing through 100 µl of buffer T50 (Fig. 2-5b).

20. Add 30 µl of biotinylated DNA (50 pM in an appropriate buffer). Adjust the concentration as necessary. See Protocol 4, Imaging Single Molecules, for further details on DNA immobilization.

    DNA sticks to the PEG surface nonspecifically if the pH is lower than 7.4.

Protocol 4

Imaging Single Molecules

This protocol describes the imaging of single molecules, with emphasis on distinguishing molecules of interest from impurities.

MATERIALS

CAUTION: See Appendix for appropriate handling of materials marked with <!>.

Reagents

Bovine serum albumin (BSA; New England Biolabs)
Buffer T50 (10 mM Tris-HCl [pH 8.0], 50 mM NaCl)
Catalase (from bovine liver; Roche Applied Science)
Cy3-labeled biotinylated DNA molecules (50 pM)
D-glucose (dextrose monohydrate; Sigma-Aldrich) or β-D-glucose
Glucose oxidase (from *Aspergillus niger* [Type VII]; Sigma-Aldrich) <!>
β-Mercaptoethanol (14 M; βME; Acros Organics) <!> (Optional; see Step 1)
Trolox (±-6-hydroxy-2,5,7,8-tetramethylchromane-2-carboxylic acid; Sigma-Aldrich) <!>

Prepare a stock solution (~2 mM) of Trolox by dissolving 30 mg of Trolox powder in 10 ml of H_2O at room temperature. Vortex for 1 minute. Filter the solution with a 0.2-μm syringe filter. Measure the absorption spectrum at 290 nm (extinction coefficient 2350 ± 100 M^{-1} cm^{-1}) to estimate the concentration. Trolox results in a drop in pH. Add NaOH to achieve proper pH. Higher solubility can be achieved by dissolving Trolox in a solution with neutral pH rather than in pure H_2O. The solution is stable for at least 15 days when stored in the dark at 4°C.

Equipment

Filter (0.2-μm syringe; Nalgene)
Spectrophotometer
Vortex mixer

METHODS

1. Prepare an oxygen scavenger system that consists of 0.4% w/v β-D-glucose or 0.8% w/v D-glucose, 1 mg/ml (165 U/ml) glucose oxidase, and 0.04 mg/ml (2170 U/ml) catalase. Add the glucose to a buffer stock solution, as it can be stored long term without degradation. Prepare 100 × "gloxy" solution (a mixture of glucose oxidase and catalase) as follows:
   i. Add 20 μl of 0.2 mg/ml catalase to 80 μl of buffer T50.
   ii. Add 10 mg of glucose oxidase to the mixture. Mix the solution by tapping (do not vortex).
   iii. Centrifuge for 1 minute.

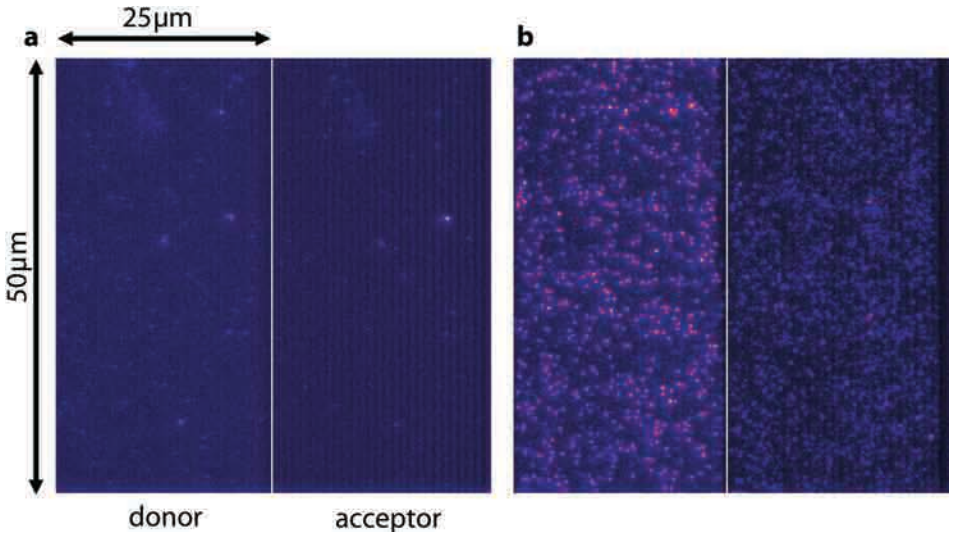

FIGURE 2-11. Single-molecule image. (*a*) The image from a blank chamber. The image is split into donor and acceptor channels, each 25 μm x 50 μm. A few fluorescent debris molecules are visible. (*b*) Shown are Cy3 molecules immobilized on the same chamber which are distinctly brighter than the debris molecules.

iv. Collect the supernatant and store it at 4°C until use (up to several months, if needed).

v. Add the gloxy to the buffer solution just before measurements are made and minimize exposure of the solution to air (see Protocol 3).

The reaction by the oxygen scavenger system generates an acid. Therefore, the solution becomes very acidic over a long time period, if the sample is allowed to equilibrate with air. Proper practice of Step v greatly reduces this problem.

2. To further improve the photostability of Cy dyes, add a triple-state quencher such as Trolox (preferred; higher than 1 mM) or 140 mM βME.

3. Image the blank chamber surface with buffer T50 (or with the imaging buffer) (Fig. 2-11a). Immobilize 50 pM Cy3-labeled molecules via biotin-(neutr)avidin conjugation (see Protocol 3, Preparing Sample Chambers). Compare the resulting density with that of the blank sample obtained with the same excitation intensity and same buffer (Fig. 2-11b). Usually, the debris molecules are not as bright as Cy dyes. Unless both the density and intensity of the debris molecules are high, the surface is regarded as clean enough for the sm-fluorescence experiment. (See Troubleshooting.)

4. Single-molecule experiments with low surface density can give misleading results because contributions of impurities can be significant. Lower the relative concentration of impurities by adding a good number of single molecules. There should be ~200 molecules on a 25 μm x 50 μm imaging area. Add 0.1 mg/ml BSA to buffer T50 to prevent the loss of precious samples of sub-nM concentrations to the surfaces of tubes and pipette tips. (See Troubleshooting.)

5. Once a desired surface density is achieved, wash out the unbound sample with buffer T50 to prevent further binding.

If the sample is too dense, more than one molecule can be found under the same spot or nearby, making the interpretation difficult. Even with a relatively low concentration sample, a small fraction of time traces can contain contributions from more than one molecule, thus giving unusual signatures.

TROUBLESHOOTING

Problem: The density and intensity of debris molecules are high.
[Step 3]
Solution: The following are possibilities:

1. The surface was not cleaned properly. Clean the surface carefully.
2. The assembled chamber was kept too long. Do not keep the chambers for longer than about 1 week.
3. The double-sided tape was dirty. Use clean tape.
4. The chemicals used for immobilization and imaging were dirty. Replace them.
5. The amino silane was contaminated (if it was a PEG-coated surface). Replace it.

Problem: The desired concentration of molecules on the surface is not achieved even with >1 nM solution.
[Step 4]
Solution: It is likely that a biotinylated sample or the chemicals and the proteins used for immobilization were not properly prepared (e.g., vortexing a protein such as neutravidin with a normal lab agitator easily inactivates the protein).

Protocol 5

Objective-type TIR Microscopy: Excitation

This protocol describes objective-type TIR microscopy (excitation), including setup of the laser beam and epifluorescence microscopy, and conversion of the latter into TIR.

MATERIALS

CAUTION: See Appendix for appropriate handling of materials marked with <!>.

Equipment

Beam expander (a pair of lenses)
Dichroic mirror (long-pass, 550-nm-cutoff wavelength; Chroma Technology)
Dichroic mirror (long-pass, 645-nm-cutoff wavelength; Chroma Technology) (optional)
Laser (green; 532 nm [Nd:YAG], 75–150 mW; Coherent, LaserQuantum, Newport, CrystaLaser) <!>
Laser (red; 633 nm, HeNe, 25–35 mW; Melles Griot) (optional; see Step 6) <!>
Lens (BK7 plano-convex, 2″ diameter, 300-mm focal length; Thorlabs)
Micrometers (2; 1″ travel translation stage; Thorlabs)
Mirrors (2; broadband dielectric, 2″ diameter; Thorlabs)
Objective lens (1.4 NA oil immersion, 100×, UPlanSApo; Olympus)

METHODS

1. Expand a laser beam so that its waist becomes 20–25 mm wide. The optics is shown in Figure 2-12.

   For example, if the laser beam is 2 mm wide, expand it 10 times by using a combination of 10- and 100-mm focal length plano-convex lenses.

2. To set the beam pathway, use a 2″ mirror (M) to reflect the widened beam through the back port of the microscope (which has a 550-nm-cutoff wavelength, long-pass dichroic mirror installed) in such a way that the beam enters the objective exactly perpendicular to the plane of the objective.

3. To converge the beam, place a 300-mm focal length plano-convex lens (XY) in the beam pathway. The distance between the lens XY and the objective should be the focal length of the lens XY, i.e., 300 mm. Typically, the lens XY is placed only a couple of inches away from the back port of the microscope if the microscope is IX71 (Olympus) without any accessories at the back port and if the beam is well-collimated in Step 1.

   A small error of a few centimeters in the distance does not significantly affect the overall quality of the setup.

4. Set up epifluorescence microscopy as follows:

   i. Since the horizontal and vertical positions of the lens XY are critical, mount the lens XY on a pair of micrometers. Adjust the two micrometers to achieve epifluorescence

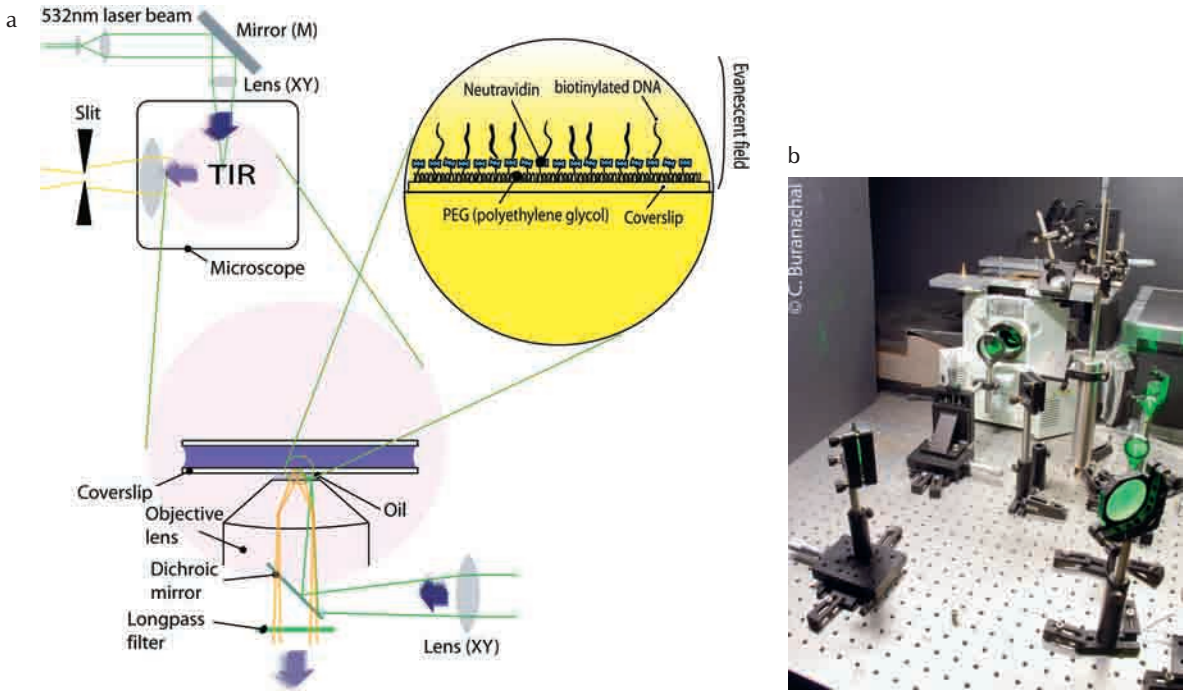

FIGURE 2-12. Objective-type TIR microscopy. (*a*) The schematic shows how the TIR occurs at the interface between a coverslip and water (side view). (*b*) The photo shows how the expanded beam is introduced into a microscope through a back port.

microscopy. A concentric pattern should come out of the objective, straight to the top. If the pattern is skewed, go back to Step 2, and correct the incident angle of the beam by moving the position of mirror M and the height of the beam as suggested.

ii. Install the optics for emission (see Protocol 6).

iii. Place a sample chamber that contains immobilized Cy3-labeled molecules in the microscope setup. Even with epifluorescence microscopy, the single molecules should show up against a high background signal.

5. To convert epifluorescence to TIR microscopy, adjust the "vertical" position of the lens XY until the beam coming out of the objective is tilted 90°. (If a slit in the emission part is placed vertically, adjustment in the vertical direction leads to the maximum view of the excitation area.) During this procedure, watch how the single-molecule image changes. When the epifluorescence excitation is changed into TIR, the background around the single molecules decreases significantly; at the same time, the Cy3 single molecules become brighter. If the position of the lens XY is further changed, all the signal suddenly disappears.

6. (Optional) Install a red laser to visualize acceptor molecules directly. Install a dichroic mirror of 645-nm-cutoff wavelength.

   This is useful when checking the presence of acceptor molecules, and excitation via epifluorescence microscopy is adequate for this purpose.

Protocol 6

Objective-type TIR Microscopy: Emission

This protocol describes the preparation of a fluorescent bead sample and the setup for objective-type TIR microscopy (emission).

MATERIALS

Reagents

Fluorescent beads (FluoSpheres carboxylate-modified microspheres, 0.2 μm, crimson fluorescent [625/645], Invitrogen)
Tris-HCl (1 M, pH 8.0)

Equipment

Bandpass filter (transmitting the light of 680 nm ± 20 nm; Chroma Technology) (optional for acceptor direct excitation; see Step 6)
Bandpass filters to reduce cross talk (optional; see Step 7)
Dichroic mirror (long-pass, 630–645 nm cutoff wavelength; Chroma Technology)
Filter (long-pass, 550-nm cutoff wavelength; Chroma Technology)
Filter holder (to fix the dichroic mirror; Thorlabs)
Glue
Lens (visible achromat doublet, 2″ diameter, 100- and 150-mm focal length; Thorlabs)
Mirrors (2; broadband dielectric, 2″ diameter; Thorlabs)
Razor blades (2)
Slide (glass)

METHODS

1. Prepare a fluorescent bead sample as follows:
   i. Dilute fluorescent beads by a factor of 500 with 1 M Tris-HCl (pH 8.0).
   ii. Inject the solution into a sample chamber (see Protocol 3, Preparing Sample Chambers) made so that the beads adhere to the imaging surface made of untreated glass.
   iii. For long-term use, seal the holes.
2. Set the beam pathway as follows:
   i. Place a fluorescent bead sample on the microscope and send the fluorescence signal to a side port. Identify an image plane that is a few centimeters outside a side port (Fig. 2-9a,b).
   ii. Place an achromat (L1; f, 100 mm) 100 mm away from the image plane.
   Even if the distance is correct (i.e., the beam is well collimated), the size of the beam waist will change after L1 since the image from the side port is not a point.
   iii. Place a mirror (M1) where the beam becomes the tightest.

3. To image on the CCD camera, place the other achromat (L2; f, 150 mm) about 5″ away from M1. Reflect the beam with the other mirror (M2), and install the camera 150 mm away from L2. Make sure that the camera is in the proper focal plane by comparing the images from an eyepiece and from the CCD screen. If the distance between L2 and the camera is far from 150 mm, the beam is not well collimated by L1.

   The emission beam should travel straight through the centers of all the lenses; otherwise, geometric aberration deforms the image of single molecules. Therefore, it is necessary that the side port, the camera, and the lenses all be the same height.

4. Prepare a vertical slit about 2.5 mm in width by gluing two razor blades to a glass slide. After properly mounting it, slide the slit into the image place determined in Step 2. Adjust the angle of M2 to place the image on the left side of the CCD screen if the beam travels as shown in Figure 2-9a.

5. To split two colors, mount a dichroic mirror (DM) on a filter holder. Place the DM a few millimeters away from the M1. While adjusting the position of the DM, watch the CCD screen and determine the proper position/angle of the DM. After immobilizing the mirror mount, adjust the relative position of the donor and acceptor images by changing the angle of either the M1 or the DM. The positions of both images can be simultaneously adjusted by the M2.

   This method of splitting two colors introduces a slight aberration between Cy3 and Cy5. However, the convenience of the alignment (and the easy replacement of the dichroic mirror for the different FRET pairs) overwhelms the disadvantage.

6. Optional: When using a red laser to visualize acceptor molecules directly, insert in a bandpass filter of 680 nm ± 20 nm.

7. Optional: Add bandpass filters to reduce cross talk.

   Optimum FRET resolution requires minimal cross talk between the two detection channels; i.e., donor emission leakage to the acceptor detector and acceptor image leakage to the donor detector. The former is usually more significant because the fluorescence emission spectrum is asymmetric with a long wavelength tail. In a typical experiment using Cy3 as the donor and Cy5 as the acceptor, ~10–15% of the donor signal is detected at the acceptor channel if a dichroic mirror with a cut-off at 645–630 nm is used to split the emission based on the wavelength. The acceptor leakage to the donor is less significant. Addition of bandpass filters is often advantageous, even though the overall signal may decrease.

Protocol 7

Prism-type TIR Microscopy: Excitation

This protocol describes the setup for prism-type TIR microscopy (excitation).

MATERIALS

CAUTION: See Appendix for appropriate handling of materials marked with <!>.

Equipment

Brass collar, a plate, and a prism holder for the objective lens (home-built)
Laser (green; 532 nm [Nd:YAG], 50–75 mW; Coherent, LaserQuantum, Newport, CrystaLaser) <!>
Laser (red; 633 nm, HeNe, 25–35 mW; Melles Griot) <!> (optional; see Step 4)
Lens (BK7 plano-convex, $^1/_2$″ diameter, 50-mm focal length; Thorlabs)
Micrometers (3; 1″ travel translation stage; Thorlabs)
Mirrors (broadband dielectric, 1″ diameter; Thorlabs)
Objective lens (1.2 NA water immersion, 60×, UPlanApo; Olympus)
Prism (Pellin-Broca [fused silica, 11.0 × 20.0 × 6.4]; EKSPLA)
Thermocouple (Digital Thermometers; Omega)
Tubing
Water-circulating bath (NESLAB RTE-7 Digital One Refrigerated Bath; Thermo Scientific)

METHODS

1. Place a small Pellin-Broca prism on top of a quartz slide with a thin layer of immersion oil in between to match the index of refraction (Fig. 2-13).
2. Focus the excitation beam into the Pellin-Broca prism. With a shallow incident angle of the excitation beam (<23°), the TIR at the interface between the quartz slide and aqueous imaging buffer is achieved.
3. Control the location and size of the excitation area by the position of the lens (f, 50 mm). It is important that the prism holder be mounted and fixed relative to the body of the microscope so that the prism and the excitation beam do not move when the sample is laterally translated to image different sample areas.
4. Optional: Install a red laser to visualize acceptor molecules directly.
5. Regulate the temperature of the sample with a water-circulating bath (NESLAB RTE-7 Digital One Refrigerated Bath) which flows to tubing in contact with the following:
   i. a home-built brass collar on the objective
   ii. a plate that holds the sample cell
   iii. metal pieces holding the prism (Fig. 2-13c,d).
6. Measure the temperature with a thermocouple sandwiched between a quartz slide and coverslip and placed on the microscope in place of the sample.

   The error in temperature measurement is estimated to be less than 1°C.

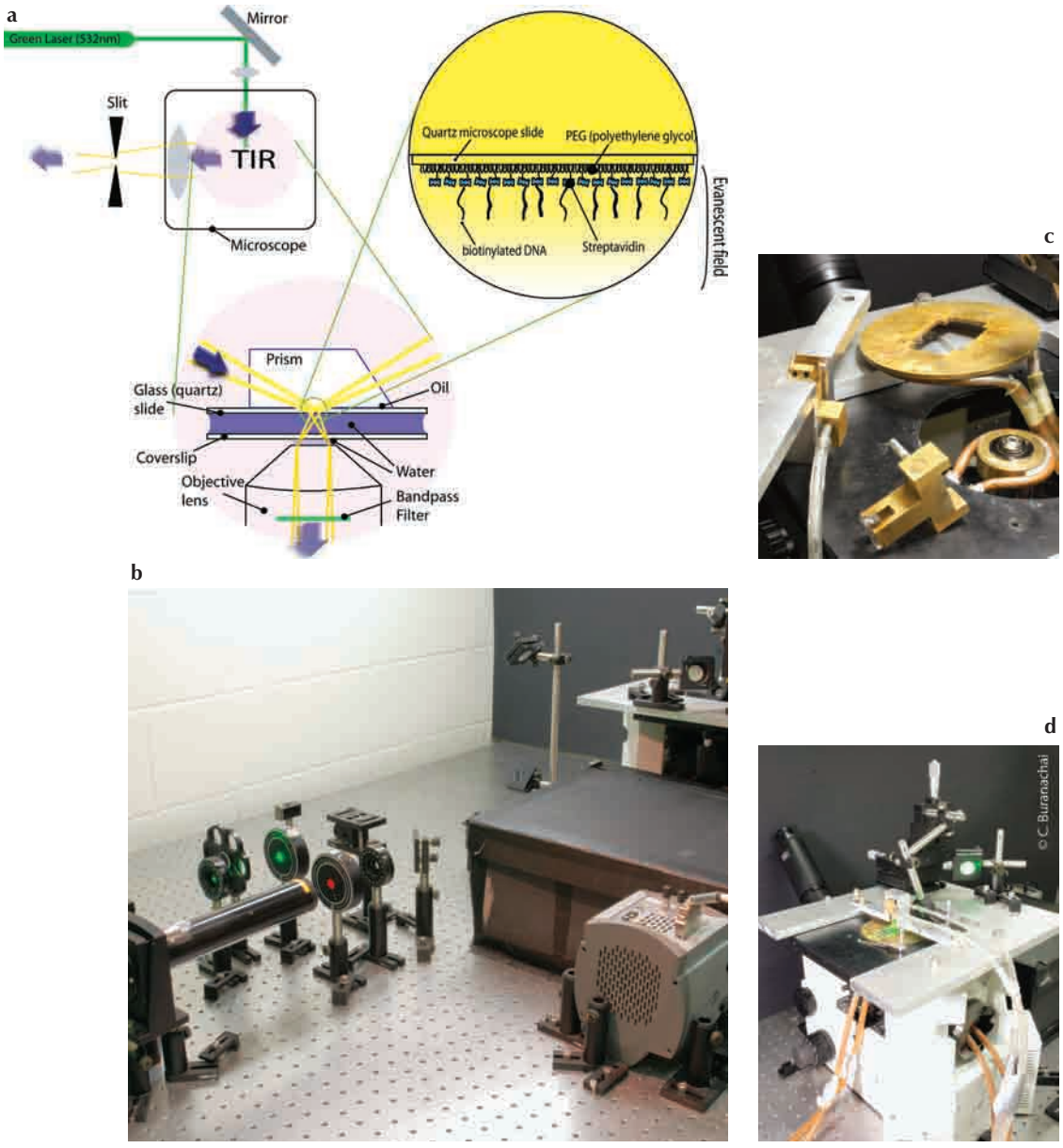

FIGURE 2-13. Prism-type TIR microscopy. (*a*) The schematic shows how the TIR occurs at the interface between a quartz slide and water (frontal view). (*b*) The photo is a bird's eye view of the excitation optics. (*c*) Components used for temperature control: a prism holder (*bottom, center*), its securing bar (*left*), a stage plate that holds the sample cell (*top*), and a home-built brass collar on the objective (*center*). (*d*) The microscope equipped with the components listed in *c* and tubing.

Protocol 8

Prism-type TIR Microscopy: Emission

Follow Protocol 6, Objective-type TIR Microscopy: Emission, with the adjustments described here. To match the size of molecules on the CCD screen with that of the objective-type TIR microscopy, use 2.5x magnification instead of 1.5 (since the water-immersion objective lens is 60x, not 100x). Therefore, use an achromat with f = 250 mm instead of one with f = 150 mm, and use a 1.5-mm-wide slit instead of a 2.5-mm-wide slit.

ACKNOWLEDGMENTS

We thank Chittanon Buranachai for taking professional pictures; Salman Syed and Julia Wright for careful reading; and the following lab members for their contributions: Sungchul Hohng (three-color), Sua Myong (protein labeling), Yongsun Kim (Trolox), Sean A. McKinney (HaMMy), Rahul Roy, and Michelle Nahas. The DNA labeling protocol is from Invitrogen.

REFERENCES

Benesch R.E. and Benesch R. 1953. Enzymatic removal of oxygen for polarography and related methods. *Science* **118:** 447–448.

Blanchard S.C., Gonzalez R.L., Kim H.D., Chu S., and Puglisi J.D. 2004. tRNA selection and kinetic proofreading in translation. *Nat. Struct. Mol. Biol.* **11:** 1008–1014.

Buranachai C., McKinney S.A., and Ha T. 2006. Single molecule nanometronome. *Nano Lett.* **6:** 496–500.

Cisse I., Okumus B., Joo C., and Ha T. 2007. Fueling protein–DNA interactions inside porous nanocontainers. *Proc. Natl. Acad. Sci.* **104:** 12646–12650.

Clamme J.P. and Deniz A.A. 2005. Three-color single-molecule fluorescence resonance energy transfer. *ChemPhysChem.* **6:** 74–77.

Clegg R.M. 1992. Fluorescence resonance energy transfer and nucleic acids. *Methods Enzymol.* **211:** 353–388.

Cornish P.V. and Ha T. 2007. A survey of single-molecule techniques in chemical biology. *ACS Chem. Biol.* **2:** 53–61.

Forster T. 1948. Intermolecular energy migration and fluorescence. *Ann. Phys.* **2:** 55–75.

Ha T. 2001a. Single-molecule fluorescence methods for the study of nucleic acids. *Curr. Opin. Struct. Biol.* **11:** 287–292.

———.2001b. Single-molecule fluorescence resonance energy transfer. *Methods* **25:** 78–86.

———.2004. Structural dynamics and processing of nucleic acids revealed by single-molecule spectroscopy. *Biochemistry* **43:** 4055–4063.

Ha T., Enderle T., Ogletree D.F., Chemla D.S., Selvin P.R., and Weiss S. 1996. Probing the interaction between two single molecules: Fluorescence resonance energy transfer between a single donor and a single acceptor. *Proc. Natl. Acad. Sci.* **93:** 6264–6268.

Ha T., Rasnik I., Cheng W., Babcock H.P., Gauss G.H., Lohman T.M., and Chu S. 2002. Initiation and re-initiation of DNA unwinding by the *Escherichia coli* Rep helicase. *Nature* **419:** 638–641.

Ha T., Ting A.Y., Liang J., Caldwell W.B., Deniz A.A., Chemla D.S., Schultz P.G., and Weiss S. 1999. Single-molecule fluorescence spectroscopy of enzyme conformational dynamics and cleavage mechanism. *Proc. Natl. Acad. Sci.* **96:** 893–898.

Heyduk T. 2002. Measuring protein conformational changes by FRET/LRET. *Curr. Opin. Biotechnol.* **13:** 292–296.

Hohng S., Joo C., and Ha T. 2004a. Single-molecule three-color FRET. *Biophys. J.* **87:** 1328–1337.

Hohng S., Wilson T.J., Tan E., Clegg R.M., Lilley D.M., and Ha T. 2004b. Conformational flexibility of four-way junctions in RNA. *J. Mol. Biol.* **336:** 69–79.

Joo C., McKinney S.A., Lilley D.M., and Ha T. 2004. Exploring rare conformational species and ionic effects in DNA Holliday junctions using single-molecule spectroscopy. *J. Mol. Biol.* **341:** 739–751.

Joo C., McKinney S.A., Nakamura M., Rasnik I., Myong S., and Ha T. 2006. Real-time observation of RecA filament dynamics with single monomer resolution. *Cell* **126:** 515–527.

Laurence T.A., Kong X., Jager M., and Weiss S. 2005. Probing structural heterogeneities and fluctuations of nucleic acids and denatured proteins. *Proc. Natl. Acad. Sci.* **102:** 17348–17353.

Lee J.Y., Okumus B., Kim D.S., and Ha T. 2005. Extreme conformational diversity in human telomeric DNA. *Proc. Natl. Acad. Sci.* **102:** 18938–18943.

McKinney S.A., Joo C., and Ha T. 2006. Analysis of single-molecule FRET trajectories using hidden Markov modeling. *Biophys. J.* **91:** 1941–1951.

McKinney S.A., Declais A.C., Lilley D.M., and Ha T. 2003. Structural dynamics of individual Holliday junctions. *Nat. Struct. Biol.* **10:** 93–97.

McKinney S.A., Freeman A.D., Lilley D.M., and Ha T. 2005. Observing spontaneous branch migration of Holliday junctions one step at a time. *Proc. Natl. Acad. Sci.* **102:** 5715–5720.

Murphy M.C., Rasnik I., Cheng W., Lohman T.M., and Ha T. 2004.

Probing single-stranded DNA conformational flexibility using fluorescence spectroscopy. *Biophys. J.* **86:** 2530–2537.

Myong S., Stevens B.C., and Ha T. 2006. Bridging conformational dynamics and function using single-molecule spectroscopy. *Structure* **14:** 633–643.

Myong S., Rasnik I., Joo C., Lohman T.M., and Ha T. 2005. Repetitive shuttling of a motor protein on DNA. *Nature* **437:** 1321–1325.

Nahas M.K., Wilson T.J., Hohng S., Jarvie K., Lilley D.M., and Ha T. 2004. Observation of internal cleavage and ligation reactions of a ribozyme. *Nat. Struct. Mol. Biol.* **11:** 1107–1113.

Okumus B., Wilson T.J., Lilley D.M., and Ha T. 2004. Vesicle encapsulation studies reveal that single molecule ribozyme heterogeneities are intrinsic. *Biophys. J.* **87:** 2798–2806.

Rasnik I., McKinney S.A., and Ha T. 2005. Surfaces and orientations: Much to FRET about? *Acc. Chem. Res.* **38:** 542–548.

———.2006. Nonblinking and long-lasting single-molecule fluorescence imaging. *Nat. Methods* **3:** 891–893.

Rasnik I., Myong S., Cheng W., Lohman T.M., and Ha T. 2004. DNA-binding orientation and domain conformation of the *E. coli* Rep helicase monomer bound to a partial duplex junction: Single-molecule studies of fluorescently labeled enzymes. *J. Mol. Biol.* **336:** 395–408.

Schatz P.J. 1993. Use of peptide libraries to map the substrate specificity of a peptide-modifying enzyme: A 13 residue consensus peptide specifies biotinylation in *Escherichia coli*. *Biotechnology* **11:** 1138–1143.

Selvin P.R. 2000. The renaissance of fluorescence resonance energy transfer. *Nat. Struct. Biol.* **7:** 730–734.

Tan E., Wilson T.J., Nahas M.K., Clegg R.M., Lilley D.M., and Ha T. 2003. A four-way junction accelerates hairpin ribozyme folding via a discrete intermediate. *Proc. Natl. Acad. Sci.* **100:** 9308–9313.

Weiss S. 1999. Fluorescence spectroscopy of single biomolecules. *Science* **283:** 1676–1683.

Zhuang X. 2005. Single-molecule RNA science. *Annu. Rev. Biophys. Biomol. Struct.* **34:** 399–414.

Zhuang X., Kim H., Pereira M.J.B., Babcock H.P., Walter N.G., and Chu S. 2002. Correlating structural dynamics and function in single ribozyme molecules. *Science* **296:** 1473–1476.

Zhuang X.W., Bartley L.E., Babcock H.P., Russell R., Ha T.J., Herschlag D., and Chu S. 2000. A single-molecule study of RNA catalysis and folding. *Science* **288:** 2048–2051.